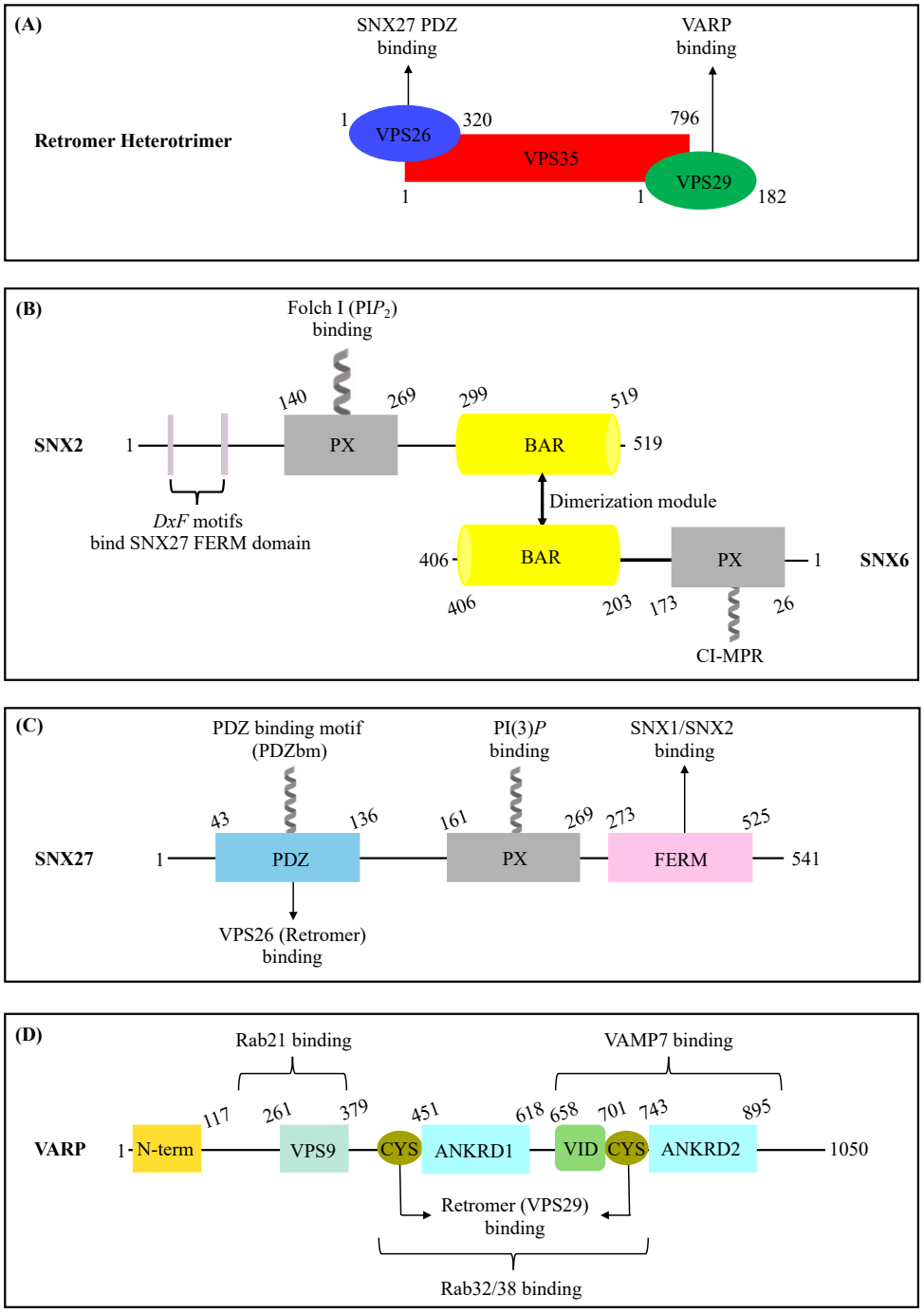

Figure S1. Domain architecture of endosomal proteins used in this study. **(A)** Domain architecture of mammalian Retromer containing three Vacuolar Protein Sorting (VPS) subunits: VPS26, VPS35, and VPS29. **(B)** Domain architecture of mammalian SNX2/SNX6 (ESCPE-1). The SNX2 N-terminus is an extended flexible region; the PX domain binds phospholipids; and the C-terminal BAR domain forms a dimer with SNX6. SNX6 contains a short and flexible N-terminus and a PX domain known to recognize a motif in CI-MPR cargo; and a C-terminal BAR domain. **(C)** Human SNX27 contains an N-terminal PDZ; central PX; and C-terminal FERM domains. The PDZ domain binds transmembrane proteins containing a PDZ binding motif (PDZbm) and the VPS26 subunit of Retromer. The PX domain recognizes PI(3)*P*, a the FERM module has been shown to bind flexible N-terminal regions of two SNX-BAR proteins, SNX1/SNX2. **(D)** Human VARP (also known as ANKRD27) domains are shown with established binding partners highlighted. Two cysteine-rich motifs (CYS) engage the VPS29 Retromer subunit, and this study establishes how the VARP N-terminus binds SNX27.

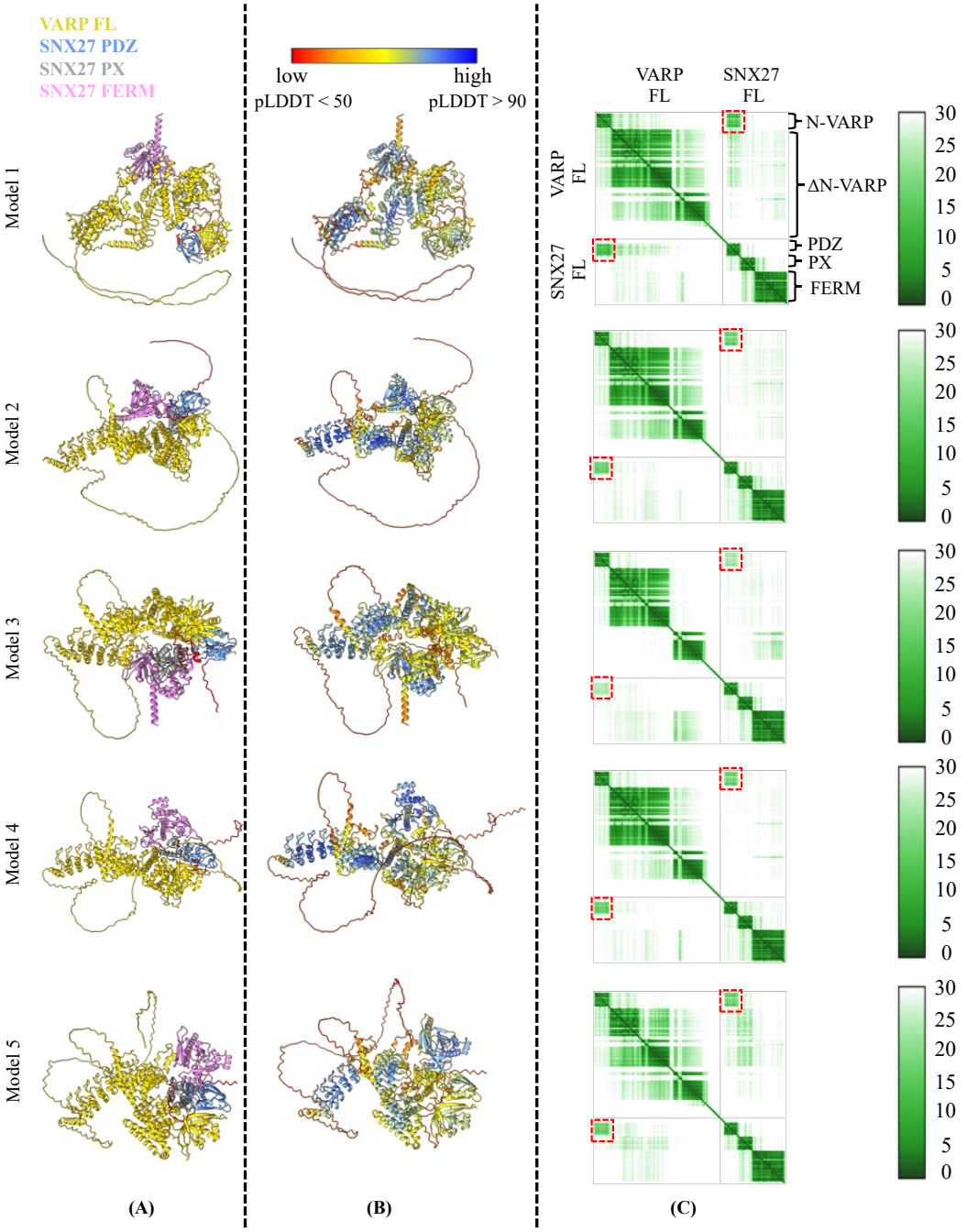

Figure S2. AlphaFold models of full-length VARP and full length SNX27. (A) Ribbon diagrams of the five top ranked models generated in AlphaFold2.3 Multimer depicting full-length VARP bound to full-length SNX27. VARP is shown in gold ribbons with SNX27 colored by domain: SNX27 PDZ in sky blue; SNX27 PX in grey, and SNX27 FERM in magenta color. **(B)** Ribbon diagrams of the top five models colored by pLDDT score. High pLDDT scores (shown in blue) reflect high confidence in local structure prediction. **(C)** For each model, the Predicted Aligned Error (PAE) score matrix is shown. Low scores (dark green color) represent high confidence in the relative position in 3D space (right column). The boundaries of protein domains can be observed in the PAE plots, including N-VARP (residues 1-117); ΔN-VARP (residues 118-1050); SNX27 PDZ (residues 43-136); SNX27 PX (residues 161-269); SNX27 FERM (residues 273-525). The predicted interaction between N-VARP and the SNX27 PDZ domain is highlighted as red dashed boxes on PAE plots.

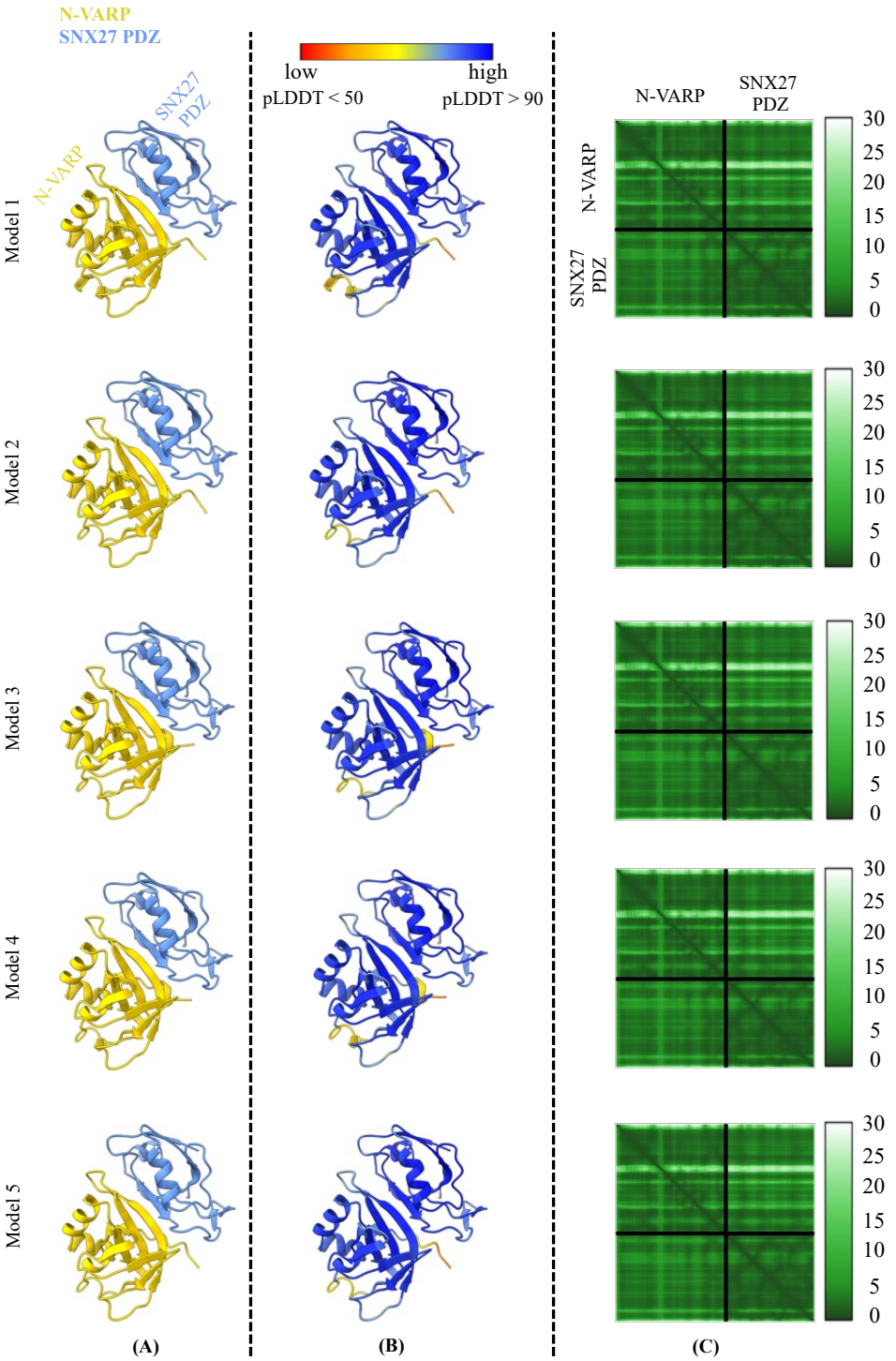

Figure S3. AlphaFold models of the VARP N-terminal globular domain with SNX27 PDZ domain. (A) Ribbon diagrams of the five top-ranked AlphaFold2.3 Multimer models depicting N-VARP bound to SNX27 PDZ. Models are colored by domain, with N-VARP in gold and SNX27 PDZ in sky blue. (B) Ribbon diagrams of top five models colored by pLDDT score; dark blue (scores >90) represents high confidence in local prediction. (C) For each model, the Predicted Aligned Error (PAE) score matrix is shown. The PAE score matrix provides low scores (deep green), signifying high confidence in the relative position in 3D space. The boundaries of protein domains (N-VARP and SNX27 PDZ) are labeled on PAE plots. Overall, AlphaFold consistently generates the same predicted model for this interaction.

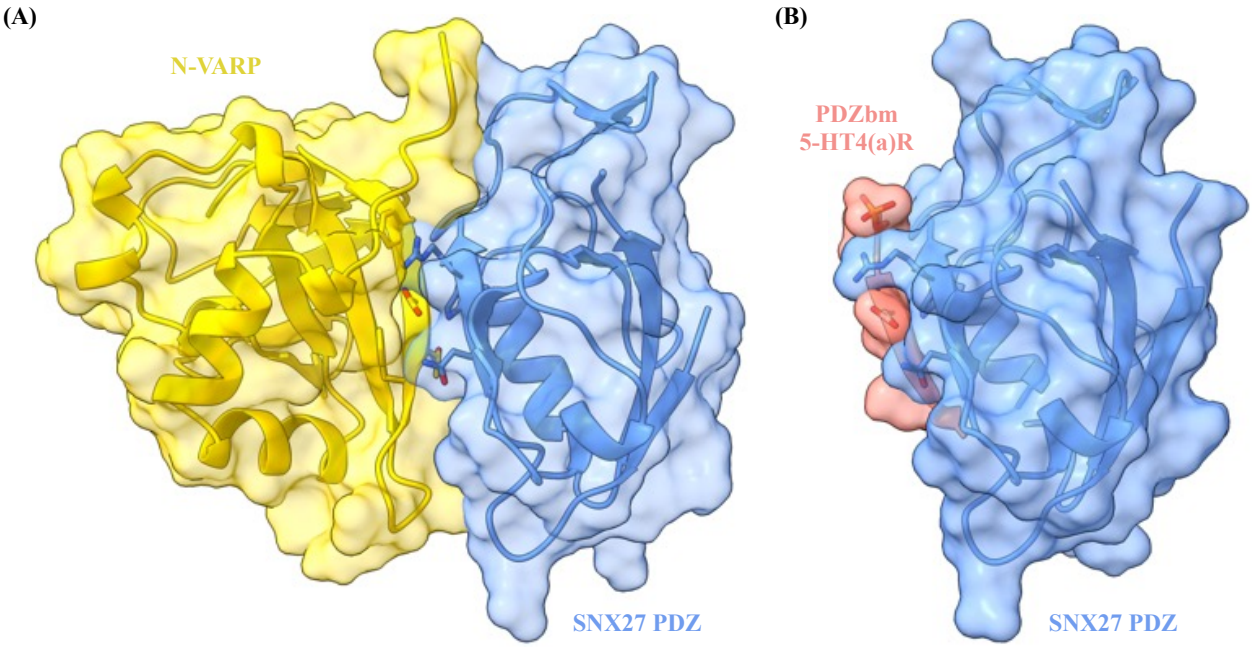

(C) Buried Surface Area comparison:

Protein-complex	**Buried Surface Area (Å²) (calculated by PISA server)**
PDB ID 5EM9 5-HT4(a)R:SNX27 PDZ	1030.0
AlphaFold2.3 Multimer N-VARP:SNX27 PDZ	1506.4

Figure S4. Comparative analysis of interactions between SNX27 PDZ and the VARP N-terminus or PDZ binding motif (PDZbm) cargo peptide. (A) Transparent surface view is shown over a ribbon diagram of VARP N-terminus (gold) and SNX27 PDZ domain (sky blue) model from AlphaFold. **(B)** Equivalent transparent surface view is shown over a ribbon diagram of the experimental X-ray structure with PDZbm peptide from 5-HT4(a)R (light red) bound to SNX27 PDZ domain (sky blue). (C) Comparison of predicted buried surface area of each structural model calculated in PISA. The interaction between N-VARP and SNX27 PDZ buries 50% greater surface area than does the PDZbm cargo peptide, in agreement with observed dissociation constants.

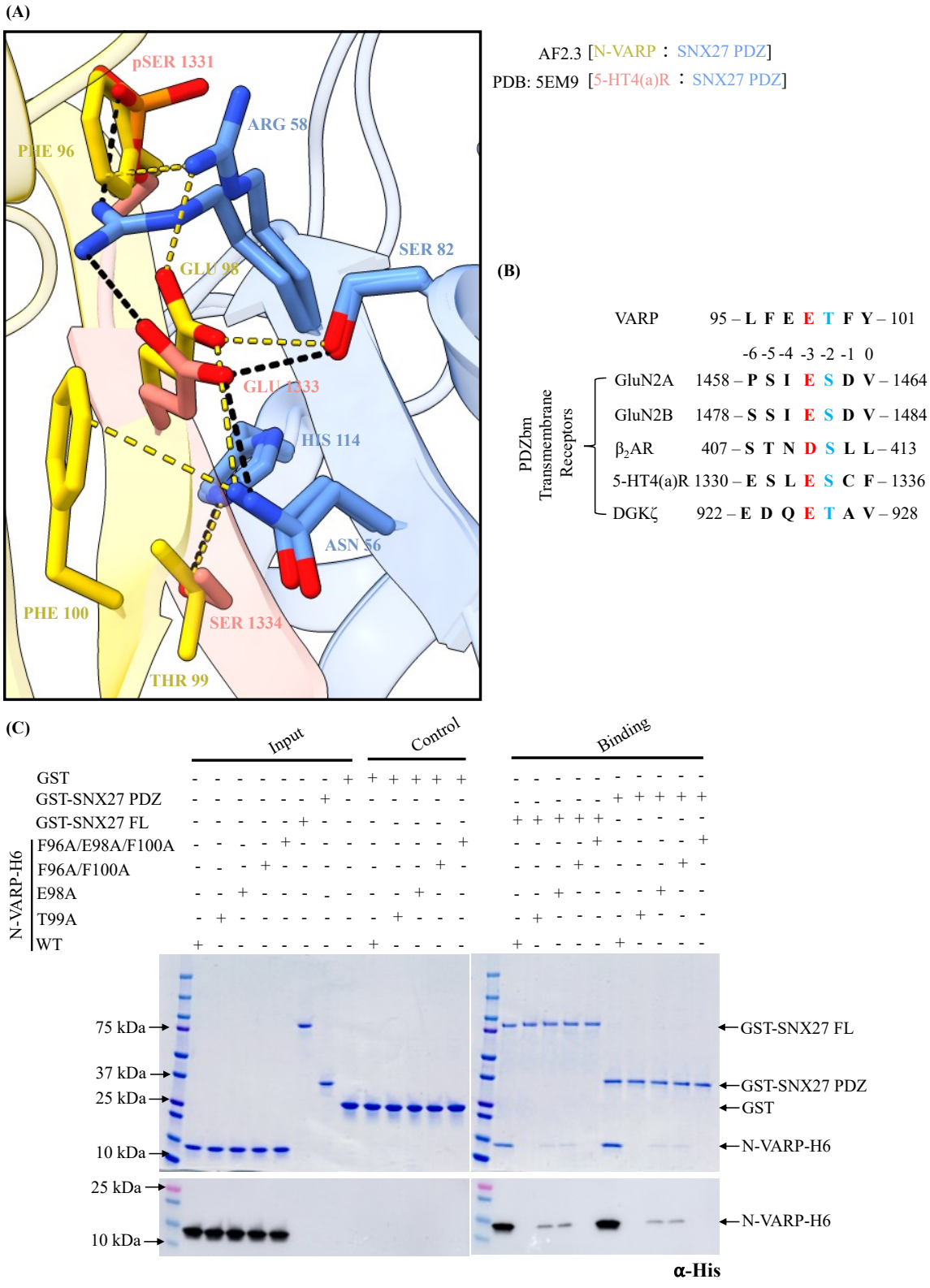
(A)
pSER 1331
ARG 58
PHE 96
SER 82
GLU 98
GLU 1333
HIS 114
ASN 56
PHE 100
SER 1334
THR 99
AF2.3 [N-VARP : SNX27 PDZ]
PDB: 5EM9 [5-HT4(a)R : SNX27 PDZ]
(B)
VARP 95 – L F E E T F Y – 101
-6 -5 -4 -3 -2 -1 0
PDZbm Transmembrane Receptors
GluN2A 1458 – P S I E S D V – 1464
GluN2B 1478 – S S I E S D V – 1484
β2AR 407 – S T N D S L L – 413
5-HT4(a)R 1330 – E S L E S C F – 1336
DGKζ 922 – E D Q E T A V – 928
(C)
Input
Control
Binding
GST
GST-SNX27 PDZ
GST-SNX27 FL
N-VARP-H6
F96A/E98A/F100A
F96A/F100A
E98A
T99A
WT
75 kDa
37 kDa
25 kDa
10 kDa
25 kDa
10 kDa
GST-SNX27 FL
GST-SNX27 PDZ
GST
N-VARP-H6
N-VARP-H6
α-His

Figure S5. The VARP N-terminus and PDZbm cargoes bind in the same pocket on the SNX27 PDZ domain. (A) Close-up view of structural superposition between C-terminal PDZbm cargo from 5-HT4(a)R (light red side chains) and SNX27 PDZ domain (sky blue; PDB: 5EM9) and the AlphaFold-predicted model of N-terminal VARP (gold) bound to SNX27 PDZ (sky blue). The superposition reveals multiple overlapping residues that mediate both interactions. Both N-terminal VARP (residues Phe96, Glu98, Thr99 and Phe100) and phosphorylated PDZbm motif (residues phospho-Ser1331, Gle1333 and Ser1334) interact with the same patch on the SNX27 PDZ domain composed of residues Asn56, Arg58, Ser82, and His114. Predicted interaction distances between the VARP N-terminus and SNX27 PDZ domain are represented as yellow dashed lines, while distances determined from the experimental structure of the PDZbm cargo motif and SNX27 PDZ domain (PDB ID: 5EM9) are shown as black dashed lines. (B) Sequence alignment and comparison of VARP N-terminus (motif: LFEETFY; residues 95−101) and multiple PDZ binding motifs in five known transmembrane receptors. The motif position numbers are assigned according to the classical type I PDZbm sequence ($D/E^{-3}–S/T^{-2}–X^{-1}–\Phi^{0}$, where Φ represents any hydrophobic residue). Residues corresponding to -2 and -3 positions are highlighted in blue and red, respectively. (C) GST pulldown experiments confirm VARP N-terminal residues from AlphaFold2 model are involved in binding. GST-tagged full length SNX27 or GST-SNX27 PDZ domain were used as baits with purified His-tagged N-terminal VARP mutant proteins (E98A; T99A; F96A/F100A double mutant; and F96A/E98A/F100A triple mutant) as prey. Representative SDS-PAGE gel stained with Coomassie blue is shown in top panel with α-His Western blot shown in bottom panel.

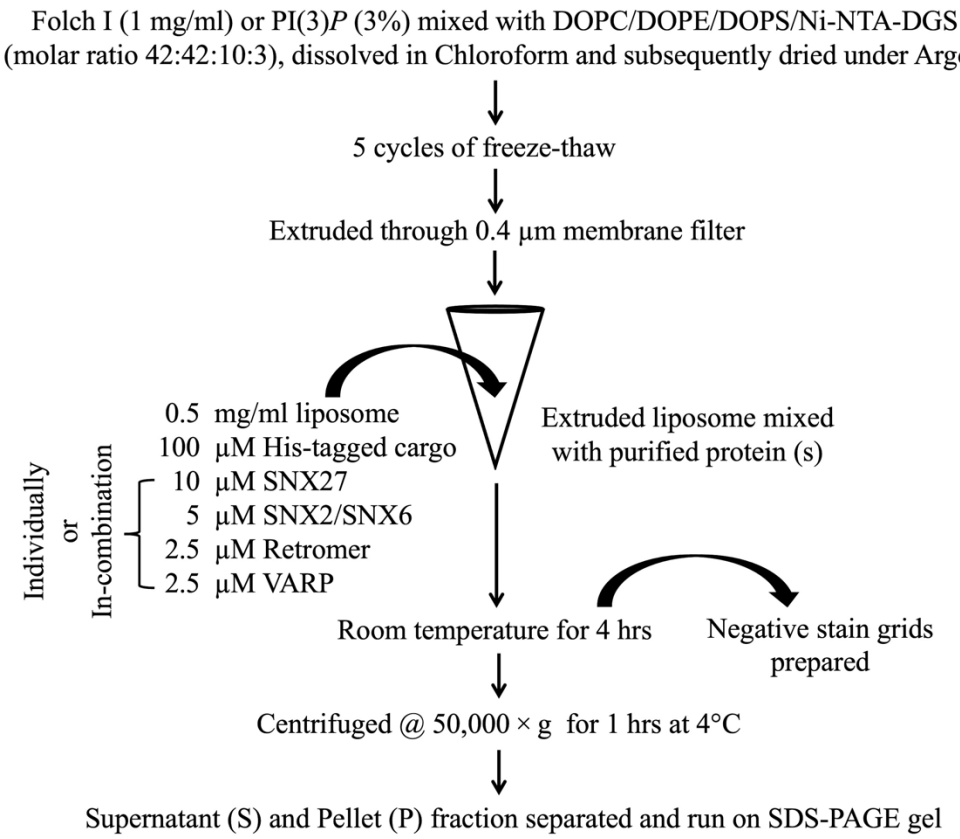

Cargo used:

- **PDZbm cargo 5HT4(a)R:** 360 – Y T V L H R G H H Q E L E K L P I H N D P E S L E S C F – 388
- **CI-MPR** cargo: 2347 – S N V S Y K Y S K V N K E E E T D E N E T E W L M E E I Q – 2375

Figure S6. Flow chart depicting steps in liposome preparation and liposome pelleting assay.

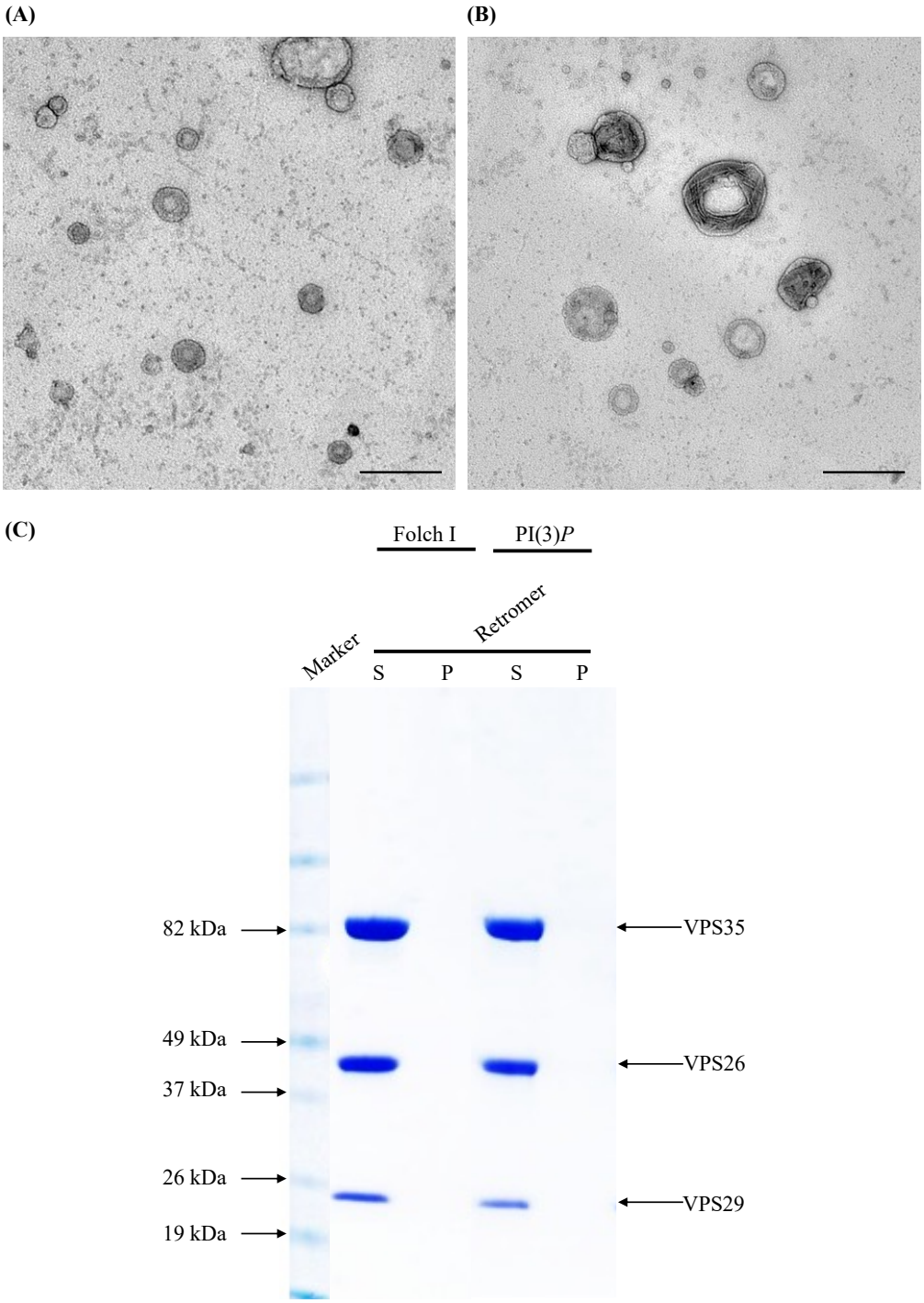

Figure S7. Control experiments to establish the reconstitution system. Representative negative stain EM images of liposomes containing (A) PI(3)*P* and (B) Folch I as controls. Liposomes containing these phospholipid compositions do not exhibit tubules. Liposomes containing either (A) PI(3)*P* or (B) Folch I were incubated with buffer (20 mM HEPES-KOH pH 7.5, 200 mM NaCl, and 1 mM Tris (2-carboxyethyl)phosphine) and visualized using negative stain EM. (Scale bar = 500 nm). (C) Liposome pelleting assay of purified Retromer complex on liposomes enriched with with Folch I or PI(3)*P*. Samples were subjected to ultracentrifugation followed by SDS-PAGE and Coomassie staining of the unbound supernatant (S) and bound pellet (P) fractions. Retromer is not recruited to membranes in the absence of cargo or SNX27.

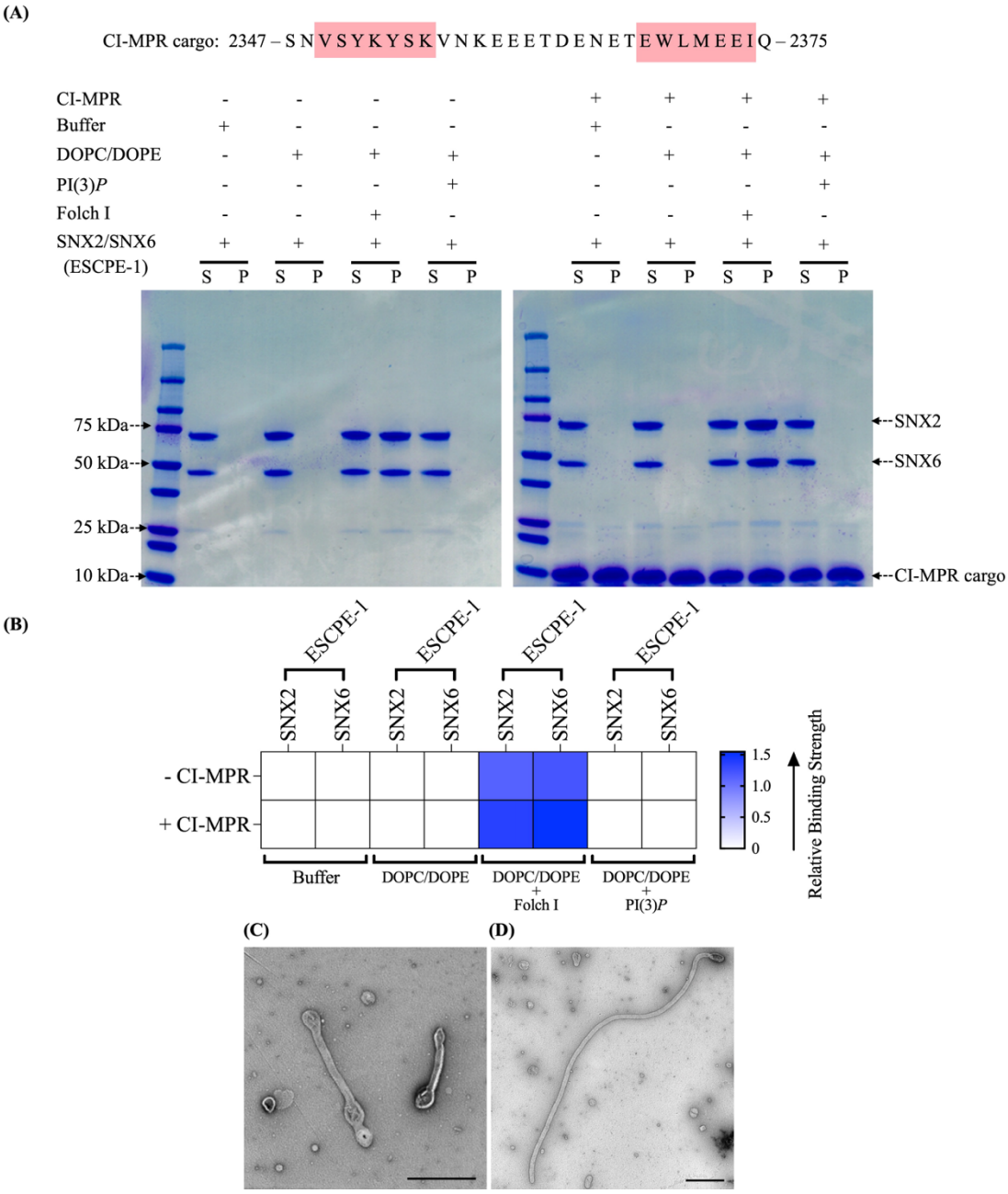

Figure S8. Membrane binding and tubulation properties of ESCPE-1 differ from those of SNX27/ Retromer. (A) Membrane binding of human SNX2/SNX6 (ESCPE-1) complex by liposome pelleting assay. Purified human SNX2/SNX6 complex was incubated with liposomes in the presence or absence of the CI-MPR cargo motif (residues 2347–2375; sequence motifs highlighted in red text). Buffer and DOPC/DOPE alone were used as negative controls to detect non-specific binding. Samples were subjected to ultracentrifugation followed by SDS-PAGE and Coomassie staining of the unbound supernatant (S) and bound pellet (P) fractions. ESCPE-1 is recruited to membranes in the presence of Folch I alone (left gel) and Folch I with CI-MPR cargo (right gel). (B) Binding of ESCPE-1 to phosphoinositide-enriched membranes visualized by SDS-PAGE was quantified by measuring relative protein band intensities (ImageJ) as in Figure 3. (C, D) Negative stain EM reveals tubulation of Folch I-enriched liposomes incubated with SNX2/SNX6 (ESCPE-1) alone (C) or in presence of CI-MPR cargo (D). Scale bars represent 500 nm.

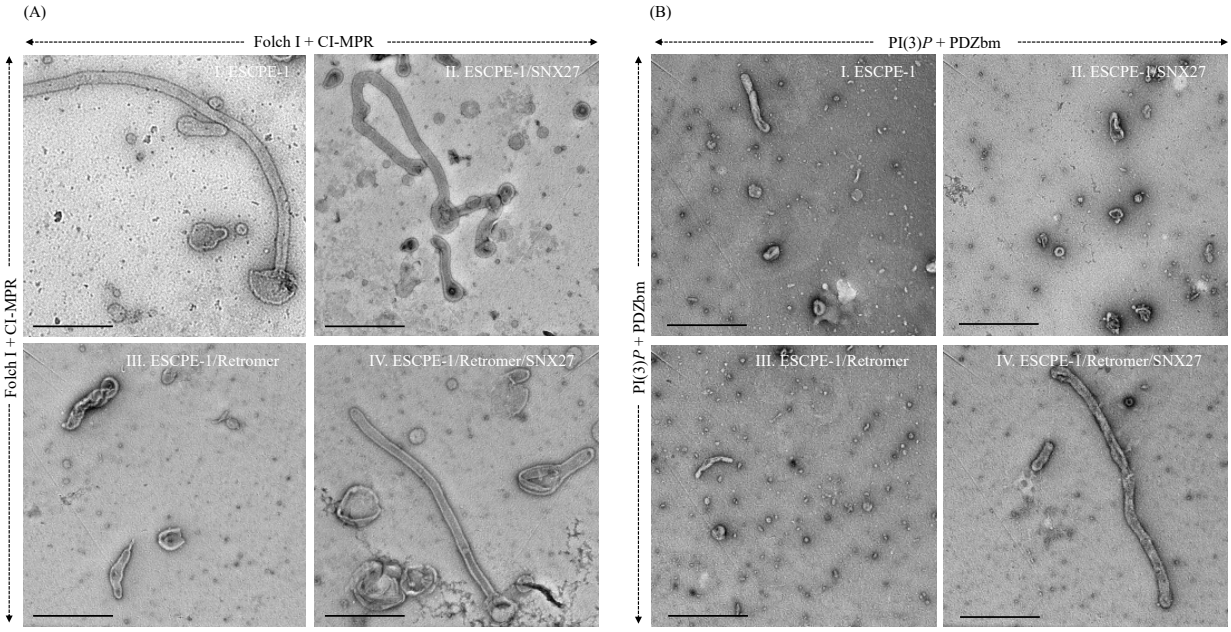

Figure S9. Morphology of membrane tubules generated by endosomal coat proteins visualized using negative stain EM. (A) Representative negative stain EM images depicting Folch I-enriched liposomes with CI-MPR cargo motif following incubation with (I) SNX2/SNX6 (ESCPE-1); (II) ESCPE-1 and SNX27; (III) ESCPE-1 and Retromer; and (IV) ESCPE-1, Retromer, and SNX27. These data further suggest ESCPE-1 drives tubulation on its own without contribution from SNX27 or Retromer. SNX27 does not effectively bind Folch-enriched membranes these conditions (see Figure 4A) or contribute to morphology. Retromer does not pellet with ESCPE-1 under these conditions (Figure 4A), and its presence may negatively impact tubule formation (panel III). **(B)** Representative negative stain EM images depicting PI(3)*P*-enriched liposomes with 5-HT4(a)R PDZbm cargo motif following incubation with (I) SNX2/SNX6 (ESCPE-1); (II) ESCPE-1 and SNX27; (III) ESCPE-1 and Retromer; and (IV) ESCPE-1, Retromer, and SNX27. ESCPE-1 is not efficiently recruited to PI3*P*-enriched membranes (see Figure 4B) and probably does not contribute to morphology observed in panel B-IV. Scale bars represent 500 nm.

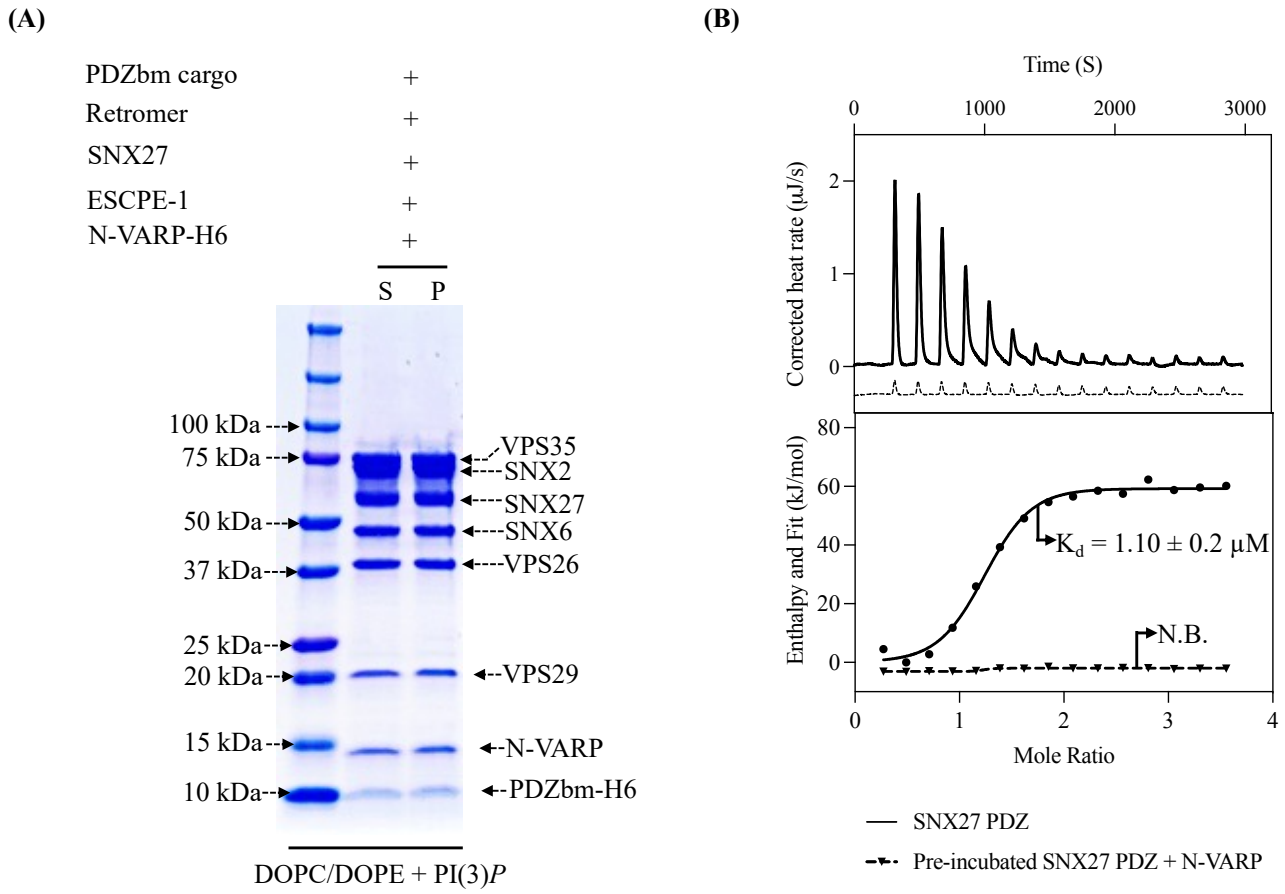

Figure S10. The VARP N-terminus recruits the supercomplex to membranes and binds in SNX27 PDZ cargo binding site. (A) Purified N-VARP protein was incubated with SNX27, ESCPE-1, and Retromer in the presence of PDZbm cargo and PI(3)*P*-enriched liposomes. All protein components are recruited to membranes in the presence of N-VARP alone. (B) Isothermal titration calorimetry (ITC) competition experiments were undertaken to establish whether N-VARP and PDZbm cargo motifs bind the same site on SNX27 PDZ. Synthesized PDZbm cargo peptide from 5-HT4(a)R was titrated into the calorimeter cell containing either purified SNX27 PDZ protein alone (dark black traces) or a 1:1 mixture of purified SNX27 PDZ and N-VARP proteins (dotted black traces). The PDZbm motif binds SNX27 PDZ with a K_D near 1 µM as established in the literature, while no detectable binding is observed when PDZbm peptide is titrated into the SNX27 PDZ/N-VARP mixture.